JOURNAL OF Materials CHEMISTRY

A variable temperature neutron diffraction study of the layered perovskite $YBaMn_2O_5$

Judith A. McAllister and J. Paul Attfield*†

Department of Chemistry, University of Cambridge, Lensfield Road, Cambridge, UK, CB2 1EW, and the Interdisciplinary Research Centre in Superconductivity, Madingley Road, Cambridge, UK, CB3 0HE

A variable temperature neutron diffraction study has been carried out on the layered perovskite $YBaMn_2O_5$ between 100 and 300 K. A broad peak indexed as (1/2, 1/2, 1) on the nuclear cell is consistent with short range Mn^{II}/Mn^{III} valence ordering. The magnetic structure below the ferrimagnetic ordering temperature of 167 K has been determined and is in agreement with a previously proposed model. Changes in lattice parameters, bond lengths and angles show evidence of an exchange striction at T_C.

Introduction

Perovskite type $Ln_{1-x}A_xMnO_3$ phases (Ln = trivalent lanthanide, A = Ca, Sr, Ba) exhibit giant magnetoresistances (GMR).[1] The features important to this phenomenon are the three-dimensional Mn—O—Mn network and Mn of mixed valency with the mean Mn oxidation state between +3 and +4, *i.e.* hole-doped Mn^{III}. This gives rise to 'double-exchange',[2] a transfer of spin-polarised electrons from Mn^{3+} to Mn^{4+}, below the Curie temperature.

A new perovskite-related Mn oxide, $YBaMn_2O_5$, was recently reported.[3] The structure has a layered arrangement with oxygen vacancies in the yttrium plane and the manganese–oxygen network consists of double layers of identical MnO_5 square pyramids linked through their apical oxygens. This structure is similar to those of $YBaCuFeO_{5+\delta}$[4] and $YBaCo_2O_{5+\delta}$.[5] Magnetic measurements on $YBaMn_2O_5$ showed a ferrimagnetic ordering temperature of 167 K with the measured ferromagnetic component of about 0.5 μ_B, this is consistent with a magnetic and valence (charge) order of Mn^{II} and Mn^{III}, as shown in Fig. 1. Each Mn^{II} is linked *via* oxygen to five Mn^{III} ions and *vice versa* which if extended over long distances would give a $\sqrt{2}a \times \sqrt{2}a \times c$ superstructure. In this study we have investigated the magnetic and crystal structures and the extent of superstructure formation in $YBaMn_2O_5$ using variable temperature powder neutron diffraction.

Experimental

A stoichiometric mixture of $YMnO_3$, BaO and MnO was used in the preparation of a 10 g sample of $YBaMn_2O_5$ for neutron diffraction. $YMnO_3$ was prepared by heating a mixture of Y_2O_3 (Aldrich 99.99%) and MnO_2 (Aldrich 99.99%) at 1350 °C for 8 h. BaO and MnO were prepared by heating BaO_2 (Aldrich 99.99%) and MnO_2 under flowing H_2–N_2 at 900 °C for 8 h. These precursors were then ground together, pressed into 13 mm pellets, wrapped in gold foil and sealed in an evacuated silica tube which was heated at 1000 °C for 4 days. This procedure was repeated twice. After each heating the tube was quenched into air to avoid possible decomposition of $YBaMn_2O_5$ on cooling. Despite many attempts with varying experimental conditions it has not been possible to prepare a phase pure sample of this phase. $YMnO_3$ and MnO were observed in the X-ray powder diffraction pattern and additional peaks subsequently observed in the neutron profile were assigned to Ba_2SiO_4 resulting from reaction with the silica tube, due to a slight rupture in the Au foil.

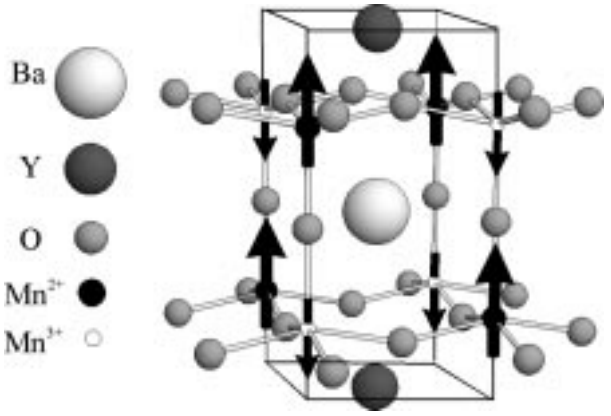

Fig. 1 Proposed[3] valence and magnetic ordering model for $YBaMn_2O_5$ showing alternating Mn^{II} with $S = 5/2$ (up) spins and Mn^{III} with $S = 2$ (down) spins

Constant wavelength neutron powder diffraction data were collected at 100, 140, 190 and 300 K on instrument D2B at the Institut Laue-Langevin, Grenoble, France. The wavelength selected for this experiment was from the (335) Bragg reflection of the Ge crystals, with $\lambda = 1.594$ Å. Rietveld refinement[6] was carried out using the General Structure Analysis System (GSAS).[7]

Results

The starting model for $YBaMn_2O_5$ in this refinement was taken from the previous X-ray study,[3] the structural parameters are given in Table 1. The impurity phases were fitted using models were taken from Yakel *et al.*,[8] Grosse *et al.*,[9] and Sasaki *et al.*[10] for $YMnO_3$, MnO and Ba_2SiO_4 respectively. A good fit to the data was obtained using a pseudo-Voigt peak shape function and a cosine Fourier series background function, despite secondary phases being present. The refined phase proportions by mass were $YBaMn_2O_5$ 32.1%, $YMnO_3$ 36.3%, Ba_2SiO_4 24.9% and MnO 6.7%. The refined $YBaMn_2O_5$ structural model is in good agreement with that of the previous X-ray diffraction study.[3] Fig. 2 shows the calculated, observed and difference plots for the 300 K data. The oxygen content was confirmed as being stoichiometric. Results of the refinement are given in Table 1 and Fig. 4 and 5 (later).

Both the 300 and 190 K data showed a broad peak at $2\theta =$

†E-mail: jpa14@cam.ac.uk

Table 1 Refinement results for $YBaMn_2O_5$[a] with e.s.d.s in parentheses

	T/K			
	100	140	190	300
χ^2	3.2	3.9	2.9	2.5
R_{WP}(%)	6.9	7.6	6.5	6.0
cell parameters				
a/Å	3.9114(2)	3.9121(2)	3.9146(2)	3.9186(2)
c/Å	7.6241(1)	7.6287(6)	7.6351(6)	7.6540(5)
atomic parameters				
U_{iso}/Å^2	0.0009(6)	0.0067(5)	0.0017(5)	0.0041(6)
Mn z	0.234(1)	0.233(1)	0.236(1)	0.236(1)
μ/μ_B	1.78(2)	1.17(6)	—	—
O(1) z	0.1868(5)	0.1870(5)	0.1858(4)	0.1870(4)
distances				
Ba—O(1)×8	3.087(3)	3.087(3)	3.096(3)	3.095(3)
Ba—O(2)×4	2.7658(1)	2.7662(1)	2.7681(1)	2.7709(1)
Y—O(1)×8	2.419(2)	2.421(2)	2.418(2)	2.426(2)
Mn—O(1)×4	1.989(7)	1.988(2)	1.995(2)	1.995(2)
Mn—O(2)×1	2.026(9)	2.034(10)	2.012(8)	2.020(8)
Mn···Mn×1	3.57(2)	3.56(2)	3.61(2)	3.61(2)
angles				
O(1)—Mn—O(1)×4	88.10(9)	88.19(10)	87.85(9)	87.97(8)
O(1)—Mn—O(1)×2	159.0(5)	159.5(6)	157.6(5)	158.3(5)
O(1)—Mn—O(2)×4	100.5(3)	100.2(3)	101.2(2)	100.9(2)
Mn—O(1)—Mn	159.0(2)	159.5(6)	157.6(5)	158.3(5)
Mn—O(2)—Mn	180	180	180	180

[a]Space group *P*4/*mmm*, Y 1(c) 1/2,1/2,0, Ba 1(d) 1/2,1/2,1/2, Mn 2(g) 0,0,z, O(1) 4(i) 1/2,0,z, O(2) 1(b) 0,0,1/2.

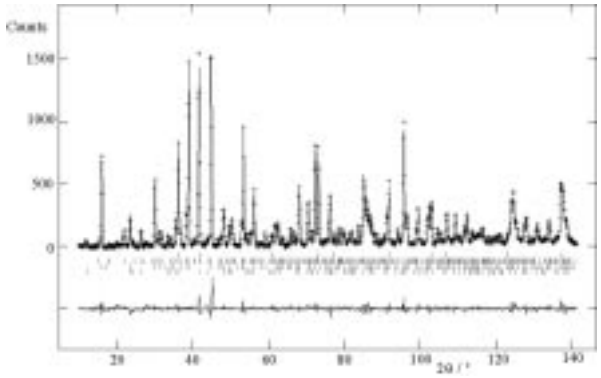

Fig. 2 Calculated, observed and difference neutron diffraction plots for 300 K. The reflection markers from bottom to top represent $YBaMn_2O_5$, $YMnO_3$, Ba_2SiO_4 and MnO respectively.

20.6°, which is not attributable to any impurity phase and can be indexed as (1/2 1/2 1) on the nuclear cell. The extent of the ordering was calculated using the Scherrer equation (1):

$$t = \frac{0.9\lambda}{\sqrt{(\Gamma_{pos}^2 - \Gamma_{std}^2)\cos\theta}} \quad (1)$$

where t is the domain size, λ is the neutron wavelength, Γ_{pos} is the full width at half maximum (FWHM) of the peak, Γ_{std} is the FWHM of a standard peak from the diffraction pattern (which is assumed to be instrumentally resolution-limited) and θ is the peak position. This gave $t \approx 50$ Å.

Below 167 K a magnetic peak appears at the (1/2 1/2 1) position showing that the magnetic cell parameters are $\sqrt{2}a \times \sqrt{2}a \times c$, where a and c are of those of the nuclear model. In the 140 and 100 K data the sharp peak due to long range magnetic order is superimposed on the broad valence order peak as shown in Fig. 3. The magnetic model in the refinement is as shown in Fig. 1, but with the Mn moments constrained to have equal magnitude, as attempts to refine the Mn^{2+} and Mn^{3+} moments independently were unsuccessful.

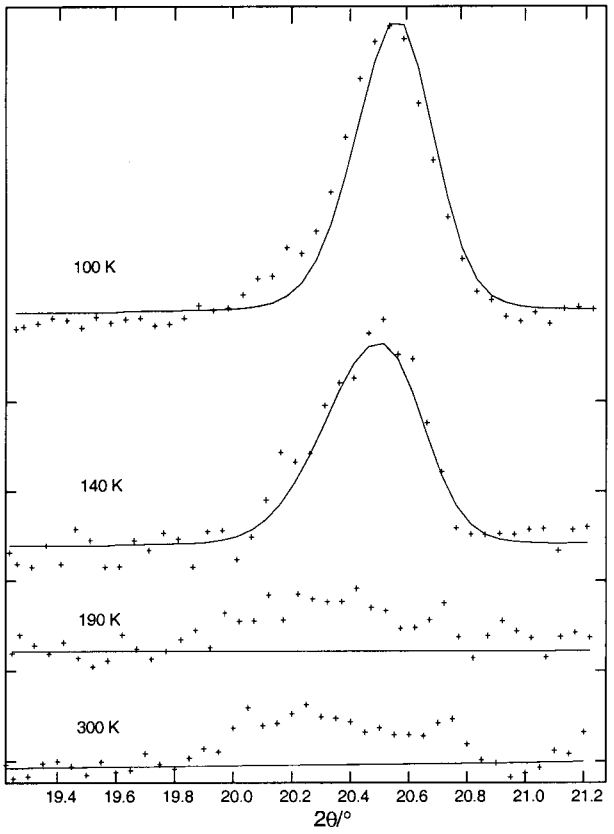

Fig. 3 Diffracted neutron intensity at the 1/2 1/2 1 position ($2\theta = 20.5°$) for $YBaMn_2O_5$ as a function of temperature. The Rietveld fits to the background and magnetic peaks are shown. The intensity scale for the 140, 190 and 300 K data is twice that for the 100 K data.

Discussion

The basic structure of $YBaMn_2O_5$ and the proposed valence and magnetic order models are confirmed by this variable

temperature neutron diffraction study. The oxygen content of $YBaMn_2O_5$ was confirmed by the refinement to be five oxygen atoms per unit cell. The presence of a broad peak above T_C and a sharp peak below, indexing on a $\sqrt{2}a \times \sqrt{2}a \times c$ supercell, give evidence for long range magnetic order below T_C but a valence ordering that extends only over *ca.* 50 Å domains.

Fig. 4 shows the variation of $YBaMn_2O_5$ lattice parameters a and c with temperature. Both parameters show a decrease with decreasing temperature which is significantly steeper about T_C. Fig. 5(a) shows the variation of Mn—O(1) and Mn—O(2) bond lengths with temperature. Mn—O(1) decreases below T_C whereas Mn—O(2) increases. These changes in bond lengths arise due to a change in the Mn—O(1)—Mn bond angle which shows an anomalous

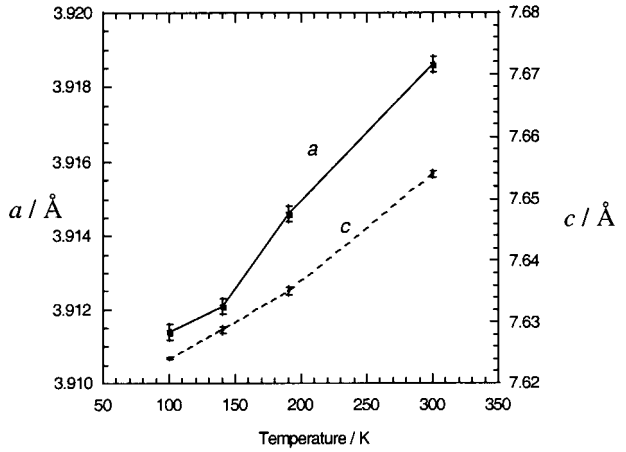

Fig. 4 Variation with temperature of a and c parameters of $YBaMn_2O_5$

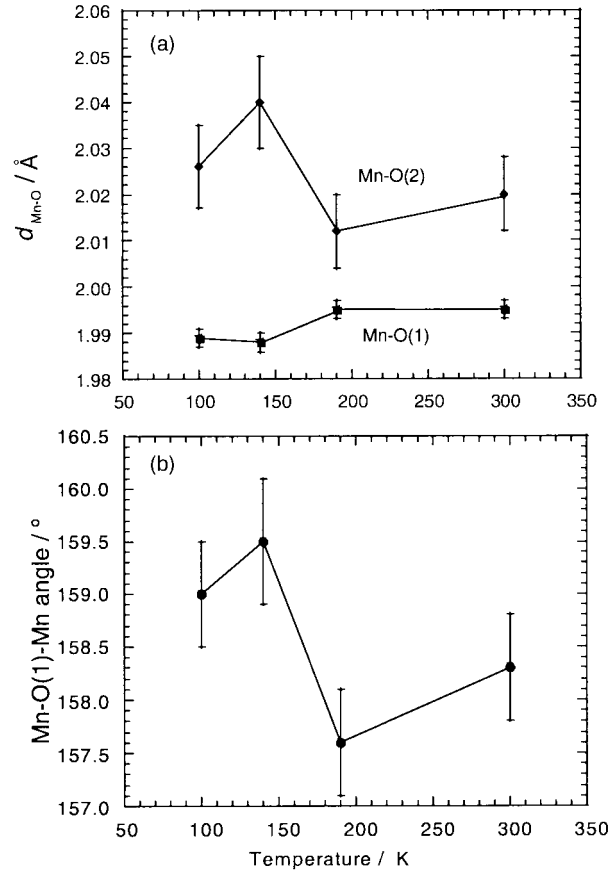

Fig. 5 Variation with temperature of (a) Mn—O(1) and Mn—O(2) bond lengths and (b) Mn—O(1)—Mn bond angle in $YBaMn_2O_5$

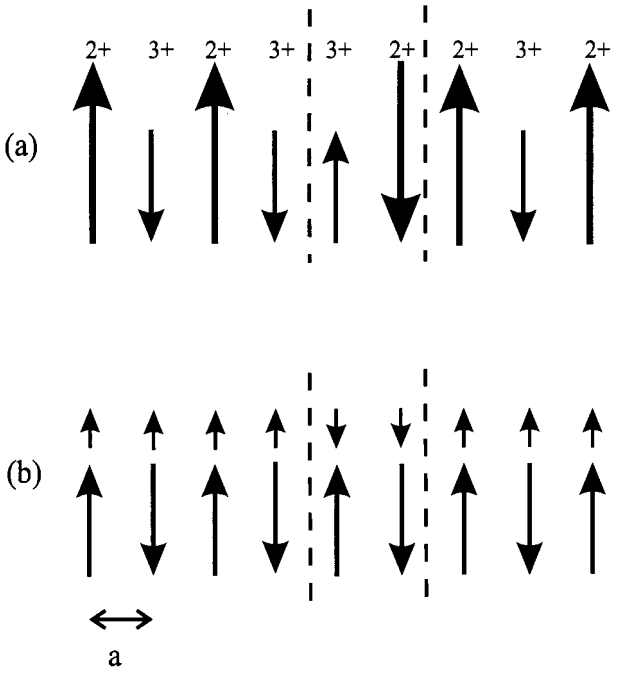

Fig. 6 Schematic one-dimensional representation of the valence and magnetic ordering of Mn^{2+} and Mn^{3+} ions in $YBaMn_2O_5$ through oxygen atoms (not shown). The broken lines represent domain walls due to disruption of the valence ordering; (a) shows the antiferromagnetic ordering of adjacent Mn^{2+} ($5\ \mu_B$) and Mn^{3+} ($4\ \mu_B$) moments, (b) shows the same situation with the moments separated into the average $4.5\ \mu_B$ and difference ($\pm 0.5\ \mu_B$) components. The former order antiferromagnetically and are unaffected by the domain walls, whereas the latter order ferromagnetically and the direction of the magnetisation is switched at the domain boundary.

increase as the temperature decreases below T_C [Fig. 5(b)]. These changes evidence an exchange striction at T_C. The changes in lattice parameters, bond lengths and angles promote superexchange *via* the Mn—O(1)—Mn bridges mainly by increasing the Mn—O(1)—Mn bond angle towards the most favourable value of 180°.

Fig. 6 shows how the valence ordering can be disrupted without affecting the long range antiferromagnetic ordering. The ideal average Mn moment is $4.5\ \mu_B$ and for the Mn^{2+} moment there is an additional $0.5\ \mu_B$ in the same direction as the average, but for the Mn^{3+} ion the extra $0.5\ \mu_B$ opposes the average. Antiferromagnetic Mn—O—Mn interactions lead to ferromagnetic ordering of the $0.5\ \mu_B$ components with unit cell $a \times a \times c$, but antiferromagnetic ordering of the average $4.5\ \mu_B$ with unit cell $\sqrt{2}a \times \sqrt{2}a \times c$. If the valence ordering is disrupted, leading to two adjacent Mn^{3+} or Mn^{2+} ions, Fig. 6 shows that the direction of the ferromagnetic component is reversed but the antiferromagnetic order is ideally unaffected. However, the average antiferromagnetic moment at 100 K is only $1.8\ \mu_B$, showing that valence disorder also causes some disruption of this order. The ferromagnetic component should give rise to weak broad magnetic reflections at the *hkl* positions of the structural cell, and so are not seen beneath the structural Bragg intensities.

In conclusion, $YBaMn_2O_5$ shows long range structural order (periodicity $a \times a \times c$) and short range valence order with a $\sqrt{2}a \times \sqrt{2}a \times c$ superstructure up to at least 300 K. Below the ferrimagnetic ordering temperature of 167 K, these structural features respectively give rise to a long range antiferromagnetically ordered component (periodicity $\sqrt{2}a \times \sqrt{2}a \times c$) and a short range ferromagnetic component that is commensurate with the basic cell.

We thank EPSRC for financial support for J.A.M. and pro-

vision of neutron facilities at the ILL, and Dr Paolo Radaelli for technical assistance with data collection.

References

1 G. H. Jonker and J. H. Van Santen, *Physica* (*Utrecht*), 1950, **16**, 337.
2 C. Zener, *Phys. Rev*., 1951, **82**, 403.
3 J. P. Chapman, J. P. Attfield, M. Molgg, C. M. Friend and T. P. Beales, *Angew. Chem*., 1996, **35**, 2482.
4 L. Er-Rakho, C. Michel, P. Lacorre and B. Raveau, *J. Solid State Chem*., 1988, **73**, 531.
5 W. Zhou, *Adv. Mater*., 1993, **5**, 735.
6 H. M. Rietveld, *J. Appl. Crystallogr*., 1969, **35**, 1.
7 A. C. Larson and R. B. Von Dreele, Los Alamos National Laboratory Rep. No. LAUR-86-748, 1987.
8 H. L. Yakel, W. C. Koehler, E. F. Bertaut and E. F. Forrat, *Acta Crystallogr*., 1963, **16**, 957.
9 H. P. Grosse and E. Tillmanns, *Cryst. Struct. Commun*., 1974, **3**, 599.
10 S. Sasaki, K. Fujino, Y. Takeuchi and R. Sadanaga, *Acta Crystallogr*., 1980, **36**, 904.

Paper 8/00605I; *Received* 22*nd January*, 1998